Determination of GISSMO Damage Parameters for High-Speed Blanking of 22MnB5 and EN AW-5754

E. Galiev[1*], M. Linnemann[1], S. Winter[1], V. Psyk[1], M. Dix[1]

[1]Fraunhofer Institute for Machine Tools and Forming Technology IWU, Reichenhainer Strasse 88, 09126 Chemnitz, Germany
*Corresponding author. Email: elmar.galiev@iwu.fraunhofer.de

Abstract

High-speed blanking (HSB) of high-strength materials, such as the steel 22MnB5, is an established method that delivers high-quality cut surfaces. Due to high shear rates, this process is associated with the formation of adiabatic shear bands (ASB) in the blanking zone. For an in-depth analysis of the effects arising in this process and to support the prototyping of blanking tools, a numerical simulation is required. For this purpose, material parameters, which are valid at elevated strain rates are necessary. In this study, the parameter identification for the GISSMO damage model is presented. For the parameter identification, a series of coupled experimental and numerical investigations were carried out on 22MnB5 and EN AW-5754 with a sheet thickness of 2 mm. The main objective was to determine the damage and failure behaviour of the investigated materials under different loading modes (or triaxialities). The resulting data was used as input for the subsequent optimisation of the parameters in LS-DYNA and LS-OPT.

Keywords

FE-Simulation, Damage model, high-speed, LS-DYNA

1 Introduction

The use of damage models to simulate complex forming processes has been increasing significantly in recent years (Gutknecht et al. 2016; Krinninger et al. 2017; Malakizadi et al. 2019). Damage model differs from conventional failure criteria in that it not only assesses the qualitative feasibility of the respective components, but also quantitativ evaluates the damage applied to the material during the forming process. This in turn is a significant advantage for following process steps such as joining (Otroshi et al. 2020; Rusia and Weihe

2020) and crash simulations (Valayil and Issac 2013; Praveen Kumar and Shrivaathsav 2019) which will further promote the use of these models in the future. Particularly interesting is the use of damage models in the simulation of cutting operations (Maranhão and Paulo Davim 2010; Zhang et al. 2017), especially of high-strength materials or at high speeds and strain rates as is case of high-speed blanking (HSB) (Schmitz et al. 2020; Winter et al. 2021; Galiev 2023).

The Johnson-Cook (JC) constitutive model (Johnson and Cook 1985) is a phenomenological formulation that extends conventional plasticity models by incorporating strain-rate sensitivity, thermal softening, and strain hardening. These features enable the model to describe characteristic material responses observed under dynamic loading conditions such as impact and penetration of metals. The three most important material reactions are strain hardening, strain rate effects and thermal softening. These three effects are combined multiplicatively in the constitutive Johnson-Cook model: The JC model is a most widely used failure model associated with conventional continuum mechanical models.

However, the JC model reaches its limits in more complex applications, especially in the simulation of high-speed blanking processes, as it does not include explicit mechanisms to account for damage and failure. To overcome these limitations, the Generalised Incremental Stress State dependent damage Model (GISSMO) was developed (Haufe et al.; Neukamm et al. 2009; Haufe et al. 2011) The most important aspect of GISSMO is the combination of damage models for crash simulation with localisation and instability models for forming applications. Especially for HSB processes, where a precise description of the material separation is crucial, GISSMO offers higher prediction accuracy than the classical Johnson-Cook model (Labinot Topilla). By combining crash simulation methods with localisation and instability models, GISSMO is particularly well suited for applications where both plastic deformation and failure mechanisms need to be captured realistically.

As part of this research, was parameter identification for GISSMO damage model by experimental and numerical inverse simulations for EN AW-5754 aluminium alloy and the press-hardened 22MnB5 steel (45 HRC) were investigated. The selection of these materials with completely different mechanical properties and fracture mechanisms enables a comprehensive evaluation of the GISSMO damage model. It also offers the opportunity to map the fracture behaviour for a broader range of materials in the context of the HSB process.

2 Methodology

2.1 Sample Geometry

The sample geometry was selected based on the recommendation of (Andrade et al. 2016) and then numerically tested in advance for suitable triaxiality ranges. The following sample types were then used for experimental investigations.

- **Tensile specimen**: Pure tensile load to determine the material behaviour under uniaxial tensile stress.
- **Shear tensile specimen 0°:** Shear load along the longitudinal axis to investigate the material behaviour under shear stress.
- **Shear tensile specimen 45°:** Shear loading at a 45° angle to the longitudinal axis to capture anisotropic effects and mixed loading conditions.
- **Notched tensile specimen:** Tensile specimen with a notch to analyse the behaviour under high triaxiality and the influence of notch effects on the damage.

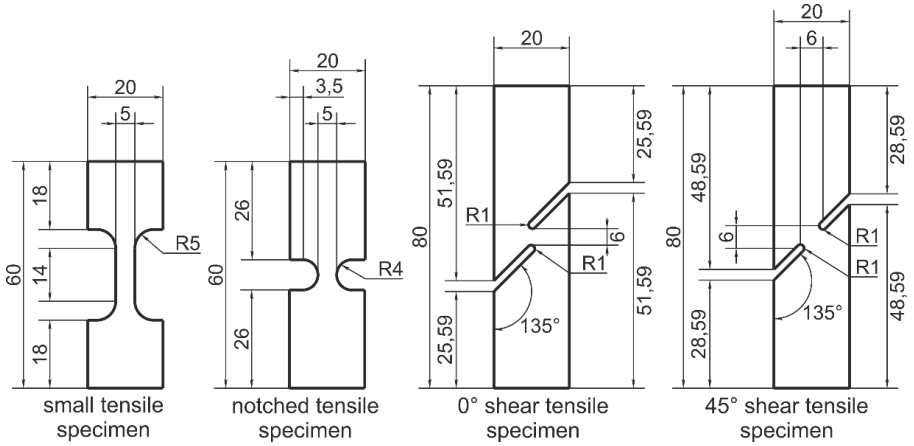

***Figure 1**: Specimen geometry causing different triaxialities in the material to identify paramters from GISSMO model*

The tensile tests were performed using a Zwick universal testing machine ZPM 1475 in accordance with ISO 6892-1:2009 (Aegerter et al. 2011). The specimens were carefully prepared and clamped in the testing machine. For the GISSMO characterisation, tensile tests leading to different triaxialities were performed. The variation of specimen geometry (**Fig.1**) allowed a comprehensive analysis of the damage behaviour of the material under different stress conditions.

2.2 FE Simulation with LS-DYNA

As part of numerical investigations in LS-DYNA, four investigated sample geometries from the experimental tests were simulated in order to later use them in an inverse simulation using LS-Opt to identify damage characteristics. In this study, the failure strain $\varepsilon_f(\eta)$and critical strain $\varepsilon_{crit}(\eta)$ were determined using LS-OPT to accurately describe material behavior within the GISSMO damage model. These parameters are essential for predicting material failure and localisation in crash and forming simulations.

In the GISSMO damage model, damage evolution is treated as a phenomenological process based on the accumulation of equivalent plastic strain in relation to stress triaxiality.

Importantly, the model does not directly simulate microstructural damage mechanisms (e.g., void nucleation or crack growth), but instead approximates their macroscopic effect through calibrated strain-based functions.

Damage (D) is computed incrementally using the equivalent plastic strain (εeq) and the failure strain εf(η), which varies with the local stress triaxiality η. Once the damage parameter D reaches a value of 1.0, complete material failure is assumed, and (if activated) element erosion may occur. The mathematical formulation is given in Equation (1).

$$D = \left(\frac{\varepsilon_{eq}^{\rho}}{\varepsilon_f(\eta)} \right)^n \tag{1}$$

Critical strain $\varepsilon_{crit}(\eta)$ marks the onset of material instability or strain localization. It is used to define the instability parameter *F* according to equation (2). When the instability parameter reaches the value on (*F*=1) damage-stress coupling is activated, leading to progressive material degradation.

$$F = \left(\frac{\varepsilon_{eq}^{\rho}}{\varepsilon_{crit}(\eta)} \right)^n \tag{2}$$

The GISSMO damage and failure model must be implemented in LS-DYNA using the keyword *MAT_ADD_EROSION and activated using the setting IDAM=1. The functions ε_f and ε_{crit} are defined as input parameters by keyword *DEFINE_CURVE and the parameters *n* and *m* are defined directly on the material card. A combination with other plasticity models available in LS-DYNA is required. For example, the classic *MAT_024_PIECEWISE_LINEAR_PLASTICITY, *MAT_133_BARLAT_YLD2000, *MAT_243_HILL_90 etc. are frequently used. In this case, MAT_133_BARLAT_YLD2000 was used because it takes into account the direction-dependent material behavior and provides better agreement with the experimental results.

To achieve statistically validated results, five samples were tested for each geometry. The target parameter for each specimen geometry for later validation and optimisation with LS-DYNA was the force-displacement curve of each specimen geometry. The force signal was provided by the Zwick tensile testing machine and the displacement was measured using a DIC camera system, with two points defined in each necking area - as shown in **Fig 2**. The elongation of the sample was evaluated by tracking the displacement of two points in the centre of the sample using HISTORY_NODE.

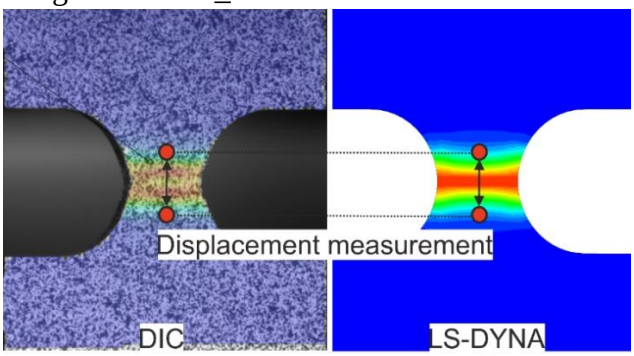

Figure 2: *Length extension measurement in the experimental DIC measurements and in the simulation*

As a first step, even before the inverse optimisation run, it was important to numerically test the selected tensile specimens in order to check the agreement between experiment and simulation in relation to the plasticity model without damage. For this purpose, the numerical model of the tensile specimens was set up in LS-DYNA using shells with ELFORM 1 and a mesh, as shown in **Fig 3**. Due to the large number of damage parameters investigated, the calculation was performed via implicit simulation in order to minimise the computational effort required as far as possible.

One side of the tested samples was fixed with 'BOUNDARY SPC SET' and the sample was pulled from the other side along the X-axis at the test speed recorded during the experimental test (2 mm/min). This corresponds to quasi-static tensile testing. In order to ensure good comparability between the measured and numerically determined data, the determination of the change of the parameter l_0 in the sample was carried out analogue to the measuring principle of DIC.

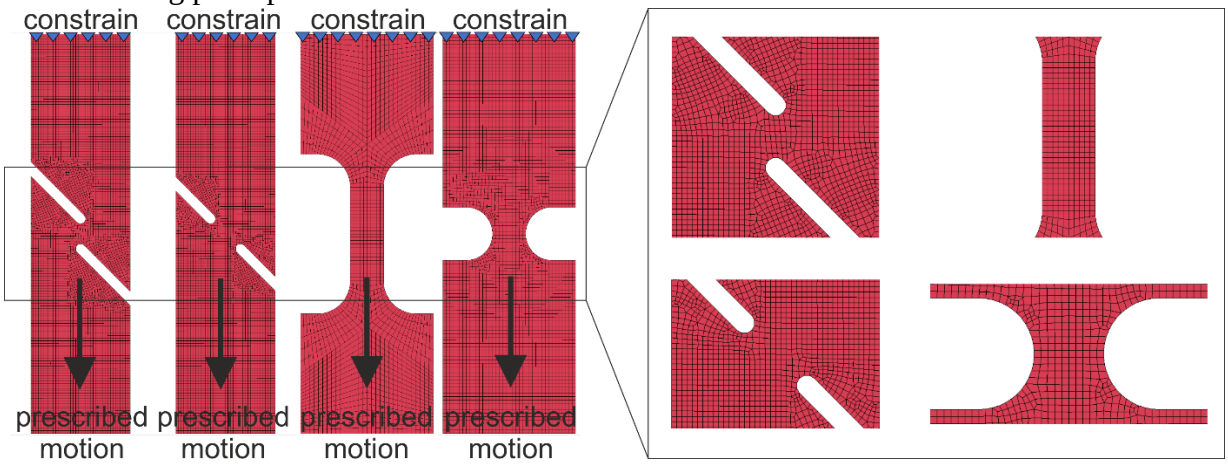

***Figure 3**: Mesh sample geometry for determining the GISSMO parameters*

2.3 FE Optimisation with LS-OPT

Based on the experimental results of the samples analysed during the tests, a parameter identification study of the GISSMO model was carried out using LS-OPT. Specifically, the selected parameters, namely failure strain and instability stain of the GISSMO model. Figure 26 start setup of variable parameters in LS-OPT were calibrated by inverse simulation. The initial parameters were identified based on experimental failure strain values within a defined range. The force-displacement curve was defined as the target variable for a good match between experimental and numerical results. After the individual calculations of the selected tensile specimens, the expected triaxiality values were also replicated in the samples., and it was possible to start the inverse optimisation in LS-OPT. The structure of the optimisation algorithm in LS-OPT is shown in **Fig 4**.

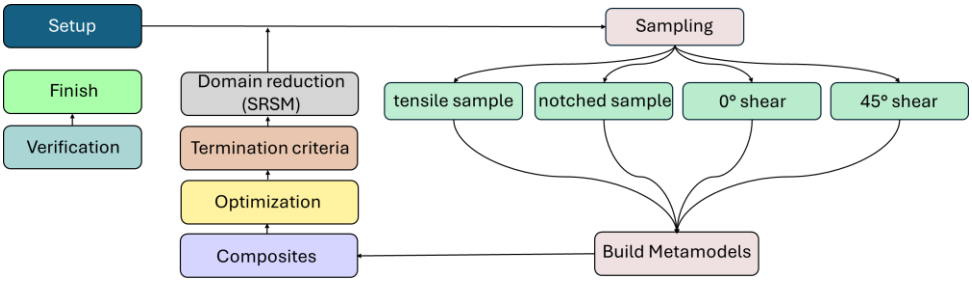

Figure 4: *Schematic of the process flow for the optimisation algorithm in LS-OPT*

Since the GISSMO parameters in LS-DYNA are primarily defined by the critical strain and failure strain as a function of stress triaxiality, an optimisation was performed using LS-OPT. The main objective of this optimisation was to calibrate the GISSMO parameters so that the simulated force-displacement curves match the experimental data as closely as possible. This ensures that the material behaviour under different loading conditions is accurately represented. As shown in **Fig.4**, the optimisation process follows a structured flow. After the sampling phase, four different specimen geometries—tensile, notched, 0° shear, and 45° shear—are evaluated, each corresponding to a specific triaxiality level. This variation is crucial for capturing the damage evolution across a wide stress state spectrum, which is essential for reliable GISSMO calibration.

A total of 20 optimisation iterations were performed, with 7 simulations per specimen geometry in each iteration, resulting in a total of 560 simulations. The use of metamodels in LS-OPT enabled efficient exploration of the parameter space and significantly reduced computational time. The domain reduction (SRSM) and termination criteria ensured that the optimisation converged towards physically meaningful and numerically stable parameter sets.

3 Results

As a result of the LS-OPT optimisation process, the force-displacement curves for the investigated specimen shapes of 22MnB5 and EN AW-5754 were mapped. Based on the agreement between numerical and experimental results, the resulting values for critical strain and failure strain were determined. For each tested sample, the experimental values were compared with the mean value of the numerical simulation. It is important to note that the determination of GISSMO parameters in this study is based on macroscopic force-displacement data without direct microstructural validation. While the onset of localization (e.g., necking) is used as a criterion for critical strain, it does not necessarily indicate the initiation of microstructural damage. Therefore, the identified parameters represent a phenomenological calibration. Future work will include microstructural analyses to support and refine the interpretation of damage evolution.

Validation results for 22MnB5 are shown in **Fig.5**. In general, good agreement is achieved for each specimen shape. For the uniaxial tensile specimen (triaxiality 0.33) and the 0° tensile specimen (triaxiality 0.05) there was a deviation for simulation in the range with transition between elastic and plastic range. This, in turn, could not be directly mapped

with some idealised boundary conditions such as machine stiffness or friction due to clamping of the sample. However, each of the selected specimens showed good agreement at the time of fracture with experiment, which is of higher significance with regard to damage modelling.

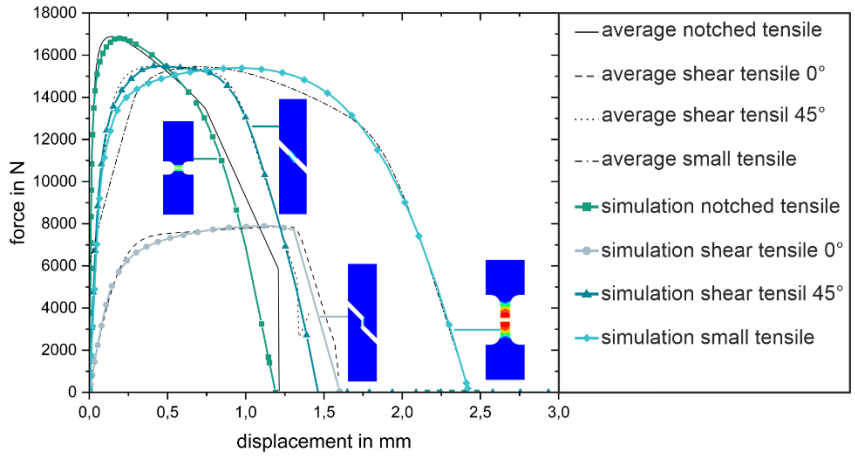

Figure 5: *Comparison of the force-displacement curves from experiment and simulation for 22MnB5 (2 mm) using the LS-OPT optimisation algorithm for tensile test, notched tensile test, 0° shear test and 45° shear test*

For the more ductile EN AW-5754 aluminum alloy the agreement of experimentally and numerically determined curves was better than for 22MnB5, as shown in Figure 6. Interesting in this case is that in the notch tensile test (triaxiality 0.66) where the general trend of the curve showed good agreement, a slight delay in the transition to failure occured. This might be improved by a more precise definition of critical strain in future work. Overall, the optimisation algorithm provided good agreement for this material.

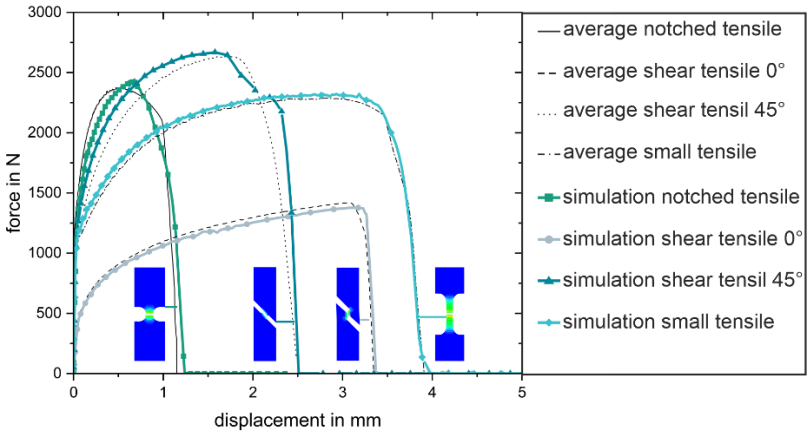

Figure 6: *Comparison of the force-displacement curves from experiment and simulation for EN AW-5754 (2 mm) using the LS-OPT optimisation algorithm for tensile test, notched tensile test, 0° shear test and 45° shear test*

4 Conclusion

In this study, the GISSMO damage parameters for the aluminium alloy EN AW-5754 and the steel 22MnB5 were calibrated with LS-OPT **(Fig.7)**. The critical strains and failure strains were determined as functions of stress triaxiality to allow a material-dependent description of the damage and failure mechanisms. The results show that both the critical strain (KD - ECRIT) and the failure strain (VD - LCSDG) exhibit a clear dependence on the stress triaxiality. The determined strain curves show that:

- **EN AW-5754** shows a significant increase in elongation at break at higher triaxialities, which indicates ductile behaviour with a strong strain hardening effect.
- **22MnB5** shows a stronger tendency towards localisation, whereby the failure strain decreases significantly at medium triaxialities, which is typical for high strength but less ductile steels.

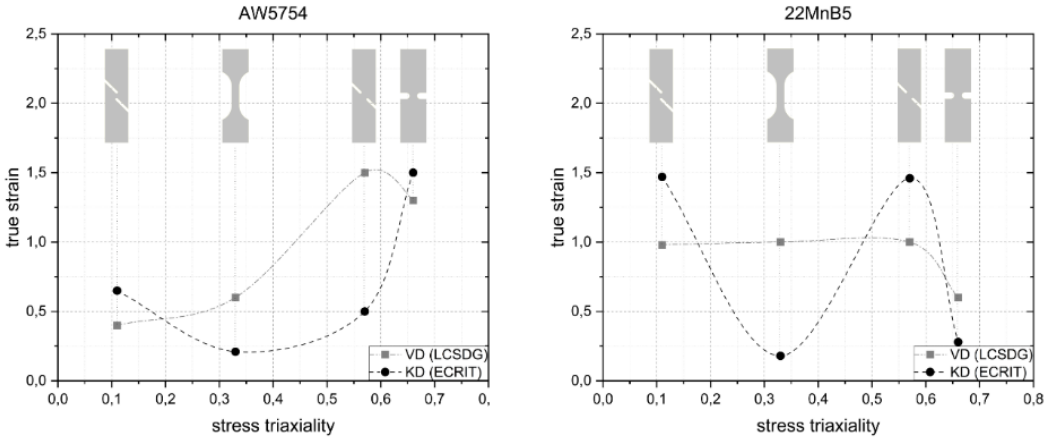

Figure 7: *The resulting GISSMO parameters for the critical strain and the failure strain of the analysed materials (22MnB5 and AW5754)*

As a final phase of the investigation of the damage parameters for 22MnB5 steel, a numerical 2D simulation was performed in LS-DYNA, as shown in **Fig. 8**. The element size in the cutting zone was 4 µm, and a high-speed blanking process was simulated with a punch speed of 10 m/s. The resulting fracture pattern showed the typical S-shape for this process and was in good agreement with the previously known experimental results. This indicates good agreement in the application of the GISSMO models for the simulation of high-speed blanking processes.

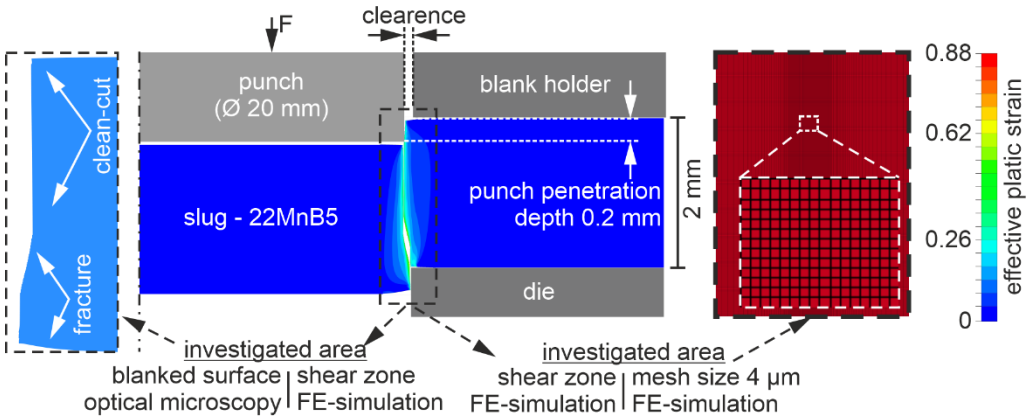

Figure 8: *Numerical 2D simulation of the high-speed blanking process (HSB) of 22MnB5 using calibrated GISSMO damage parameters*

Acknowledgements

This research was conducted as part of the DFG (Deutsche Forschungsgemeinschaft) research group FUNDAMENT 5380. We extend our sincere thanks for the support and efficient collaboration.

5 References

Aegerter J, Kühn H-J, Frenz H, Weißmüller C (2011) EN ISO 6892-1: 2009 tensile testing: initial experience from the practical implementation of the new standard. Materials Testing 53:595–603

Andrade FXC, Feucht M, Haufe A, Neukamm F (2016) An incremental stress state dependent damage model for ductile failure prediction. Int J Fract 200:127–150. https://doi.org/10.1007/s10704-016-0081-2

Galiev E (2023) Numerical and experimental study of high-speed blanking of DC06 steel. In: Sheet Metal 2023. Materials Research Forum LLC, pp 27–34. https://doi.org/10.21741/9781644902417-4

Gutknecht F, Steinbach F, Hammer T, Clausmeyer T, Volk W, Tekkaya AE (2016) Analysis of shear cutting of dual phase steel by application of an advanced damage model. Procedia Structural Integrity 2:1700–1707. https://doi.org/10.1016/j.prostr.2016.06.215

Haufe A, Neukamm F, Feucht M, DuBois P, Borvall T A comparison of recent damage and failure models for steel materials in crashworthiness application in LS-DYNA. In: 11th International LS-DYNA Users Conference, pp 6–8

Haufe A, DuBois P, Neukamm F, Feucht M (eds) (2011) GISSMO–Material modeling with a sophisticated failure criteria

Johnson GR, Cook WH (1985) Fracture characteristics of three metals subjected to various strains, strain rates, temperatures and pressures. Engineering fracture mechanics 21:31–48

Krinninger M, Opritescu D, Golle R, Volk W (2017) On the opportunities of problem- and process-adapted shear cutting simulations for effective process design. Procedia Engineering 207:1570–1575. https://doi.org/10.1016/j.proeng.2017.10.1080

Labinot Topilla ST Analysis of the Fracture Behaviour of Dual-phase Steels Using the GISSMO and Johnson Cook Models

Malakizadi A, Oberbeck JN, Magnevall M, Krajnik P (2019) A new constitutive model for cutting simulation of 316L austenitic stainless steel. Procedia CIRP 82:53–58. https://doi.org/10.1016/j.procir.2019.04.064

Maranhão C, Paulo Davim J (2010) Finite element modelling of machining of AISI 316 steel: Numerical simulation and experimental validation. Simulation Modelling Practice and Theory 18:139–156. https://doi.org/10.1016/j.simpat.2009.10.001

Neukamm F, Feucht M, Haufe A (2009) Considering damage history in crashworthiness simulations. Ls-Dyna Anwenderforum

Otroshi M, Rossel M, Meschut G (2020) Stress state dependent damage modeling of self-pierce riveting process simulation using GISSMO damage model. Journal of Advanced Joining Processes 1:100015. https://doi.org/10.1016/j.jajp.2020.100015

Praveen Kumar A, Shrivaathsav S (2019) Influence of forming parameters on the crash performance of capped cylindrical tubes using LS-DYNA follow-on simulations. Int J Interact Des Manuf 13:1215–1232. https://doi.org/10.1007/s12008-019-00552-z

Rusia A, Weihe S (2020) Development of an end-to-end simulation process chain for prediction of self-piercing riveting joint geometry and strength. Journal of Manufacturing Processes 57:519–532

Schmitz F, Winter S, Clausmeyer T, Wagner MF-X, Tekkaya A (2020) Adiabatic blanking of advanced high-strength steels. CIRP Annals 69:269–272. https://doi.org/10.1016/j.cirp.2020.03.007

Valayil TP, Issac JC (2013) Crash simulation in ANSYS LS-DYNA to explore the crash performance of composite and metallic materials. International Journal of Scientific & Engineering Research 4

Winter S, Nestler M, Galiev E, Hartmann F, Psyk V, Kräusel V, Dix M (2021) Adiabatic Blanking: Influence of Clearance, Impact Energy, and Velocity on the Blanked Surface. JMMP 5:35. https://doi.org/10.3390/jmmp5020035

Zhang Q, Zhang S, Li J (2017) Three Dimensional Finite Element Simulation of Cutting Forces and Cutting Temperature in Hard Milling of AISI H13 Steel. Procedia Manufacturing 10:37–47. https://doi.org/10.1016/j.promfg.2017.07.018